10-2016

ORM Expression Alters Sphingolipid Homeostasis and Differentially Affects Ceramide Synthase Activity

Athen N. Kimberlin
University of Nebraska - Lincoln, akimberlin1@huskers.unl.edu

Gongshe Han
Uniformed Services University of the Health Sciences

Kyle D. Luttgeharm
University of Nebraska-Lincoln

Ming Chen
University of Nebraska-Lincoln

Rebecca E. Cahoon
University of Nebraska-Lincoln, rcahoon2@unl.edu

See next page for additional authors

ORM Expression Alters Sphingolipid Homeostasis and Differentially Affects Ceramide Synthase Activity[1][OPEN]

Athen N. Kimberlin[2], Gongshe Han[2], Kyle D. Luttgeharm, Ming Chen, Rebecca E. Cahoon, Julie M. Stone, Jonathan E. Markham, Teresa M. Dunn*, and Edgar B. Cahoon*

Center for Plant Science Innovation and Department of Biochemistry, University of Nebraska-Lincoln, Lincoln, Nebraska 68588 (A.N.K., K.D.L., M.C., R.E.C., J.M.S., J.E.M., E.B.C.); and Department of Biochemistry and Molecular Biology, Uniformed Services University of the Health Sciences, Bethesda, Maryland 20814 (G.H., T.M.D.)

ORCID IDs: 0000-0001-9927-7939 (G.H.); 0000-0002-1500-9855 (K.D.L.); 0000-0003-3392-5766 (R.E.C.); 0000-0003-2829-8569 (J.M.S.); 0000-0003-2397-3131 (J.E.M.); 0000-0002-7277-1176 (E.B.C.).

Sphingolipid synthesis is tightly regulated in eukaryotes. This regulation in plants ensures sufficient sphingolipids to support growth while limiting the accumulation of sphingolipid metabolites that induce programmed cell death. Serine palmitoyltransferase (SPT) catalyzes the first step in sphingolipid biosynthesis and is considered the primary sphingolipid homeostatic regulatory point. In this report, Arabidopsis (*Arabidopsis thaliana*) putative SPT regulatory proteins, orosomucoid-like proteins AtORM1 and AtORM2, were found to interact physically with Arabidopsis SPT and to suppress SPT activity when coexpressed with Arabidopsis SPT subunits long-chain base1 (LCB1) and LCB2 and the small subunit of SPT in a yeast (*Saccharomyces cerevisiae*) SPT-deficient mutant. Consistent with a role in SPT suppression, *AtORM1* and *AtORM2* overexpression lines displayed increased resistance to the programmed cell death-inducing mycotoxin fumonisin B_1, with an accompanying reduced accumulation of LCBs and C16 fatty acid-containing ceramides relative to wild-type plants. Conversely, RNA interference (RNAi) suppression lines of *AtORM1* and *AtORM2* displayed increased sensitivity to fumonisin B_1 and an accompanying strong increase in LCBs and C16 fatty acid-containing ceramides relative to wild-type plants. Overexpression lines also were found to have reduced activity of the class I ceramide synthase that uses C16 fatty acid acyl-coenzyme A and dihydroxy LCB substrates but increased activity of class II ceramide synthases that use very-long-chain fatty acyl-coenzyme A and trihydroxy LCB substrates. RNAi suppression lines, in contrast, displayed increased class I ceramide synthase activity but reduced class II ceramide synthase activity. These findings indicate that ORM mediation of SPT activity differentially regulates functionally distinct ceramide synthase activities as part of a broader sphingolipid homeostatic regulatory network.

Sphingolipids play critical roles in plant growth and development as essential components of endomembranes, including the plasma membrane, where they constitute more than 40% of the total lipid (Sperling et al., 2005; Cacas et al., 2016). Sphingolipids also are highly enriched in detergent-insoluble membrane fractions of the plasma membrane that form microdomains for proteins with important cell surface activities, including cell wall biosynthesis and hormone transport (Cacas et al., 2012, 2016; Perraki et al., 2012; Bayer et al., 2014). In addition, sphingolipids, particularly those with very-long-chain fatty acids (VLCFAs), are integrally associated with Golgi-mediated protein trafficking that underlies processes related to the growth of plant cells (Bach et al., 2008, 2011; Markham et al., 2011; Melser et al., 2011). Furthermore, sphingolipids function through their bioactive long-chain base (LCB) and ceramide metabolites to initiate programmed cell death (PCD), important for mediating plant pathogen resistance through the hypersensitive response (Greenberg et al., 2000; Liang et al., 2003; Shi et al., 2007; Bi et al., 2014; Simanshu et al., 2014).

Sphingolipid biosynthesis is highly regulated in all eukaryotes. In plants, the maintenance of sphingolipid homeostasis is vital to ensure sufficient sphingolipids for growth (Chen et al., 2006; Kimberlin et al., 2013) while restricting the accumulation of PCD-inducing ceramides and LCBs until required for processes such as the pathogen-triggered hypersensitive response. Serine palmitoyltransferase (SPT), which catalyzes the first step in LCB synthesis, is generally believed to be the primary control point for sphingolipid homeostasis

[1] This work was supported by the National Science Foundation (grant no. MCB–1158500 to J.M.S., T.M.D., and E.B.C.).

[2] These authors contributed equally to the article.

* Address correspondence to teresa.dunn@usuhs.edu and ecahoon2@unl.edu.

The author responsible for distribution of materials integral to the findings presented in this article in accordance with the policy described in the Instructions for Authors (www.plantphysiol.org) is: Edgar B. Cahoon (ecahoon2@unl.edu).

A.N.K., G.H., J.M.S., T.M.D., and E.B.C. contributed to the conception of the research; A.N.K. and G.H. conducted most of the research; A.N.K., G.H., T.M.D., and E.B.C. analyzed data and wrote the article; K.D.L. and J.E.M. contributed to the research conception and studies on ceramide synthases; M.C. initiated the research; R.E.C. conducted mass spectrometry-based sphingolipid analyses; T.M.D. and E.B.C. supervised the project.

[OPEN] Articles can be viewed without a subscription.

www.plantphysiol.org/cgi/doi/10.1104/pp.16.00965

(Hanada, 2003). SPT synthesizes LCBs, unique components of sphingolipids, by catalyzing a pyridoxal phosphate-dependent condensation of Ser and palmitoyl (16:0)-CoA in plants (Markham et al., 2013). Similar to other eukaryotes, the Arabidopsis (*Arabidopsis thaliana*) SPT is a heterodimer consisting of LCB1 and LCB2 subunits (Chen et al., 2006; Dietrich et al., 2008; Teng et al., 2008). Research to date has shown that SPT is regulated primarily by posttranslational mechanisms involving physical interactions with noncatalytic, membrane-associated proteins that confer positive and negative regulation of SPT activity (Han et al., 2009, 2010; Breslow et al., 2010). These proteins include a 56-amino acid small subunit of SPT (ssSPT) in Arabidopsis, which was recently shown to stimulate SPT activity and to be essential for generating sufficient amounts of sphingolipids for pollen and sporophytic cell viability (Kimberlin et al., 2013).

Evidence from yeast and mammalian research points to a more critical role for proteins termed ORMs (for orosomucoid-like proteins) in sphingolipid homeostatic regulation (Breslow et al., 2010; Han et al., 2010). The *Saccharomyces cerevisiae* Orm1p and Orm2p negatively regulate SPT through reversible phosphorylation of these polypeptides in response to intracellular sphingolipid levels (Breslow et al., 2010; Han et al., 2010; Roelants et al., 2011; Gururaj et al., 2013; Muir et al., 2014). Phosphorylation/dephosphorylation of ORMs in *S. cerevisiae* presumably affects the higher order assembly of SPT to mediate flux through this enzyme for LCB synthesis (Breslow, 2013). In this sphingolipid homeostatic regulatory mechanism, the *S. cerevisiae* Orm1p and Orm2p are phosphorylated at their N termini by Ypk1, a TORC2-dependent protein kinase (Han et al., 2010; Roelants et al., 2011). The absence of this phosphorylation domain in mammalian and plant ORM homologs brings into question the nature of SPT reversible regulation by ORMs in other eukaryotic systems (Hjelmqvist et al., 2002).

Sphingolipid synthesis also is mediated by the *N*-acylation of LCBs by ceramide synthases to form ceramides, the hydrophobic backbone of the major plant glycosphingolipids, glucosylceramide (GlcCer) and glycosyl inositolphosphoceramide (GIPC). Two functionally distinct classes of ceramide synthases occur in Arabidopsis, designated class I and class II (Chen et al., 2008). Class I ceramide synthase activity resulting from the *Longevity Assurance Gene One Homolog*2 (*LOH2*)-encoded ceramide synthase acylates, almost exclusively, LCBs containing two hydroxyl groups (dihydroxy LCBs) with 16:0-CoA to form C16 ceramides, which are used primarily for GlcCer synthesis (Markham et al., 2011; Ternes et al., 2011; Luttgeharm et al., 2016). Class II ceramide synthase activities resulting from the *LOH1*- and *LOH3*-encoded ceramide synthases are most active in the acylation of LCBs containing three hydroxyl groups (trihydroxy LCBs) with VLCFA-CoAs, including primarily C_{24} and C_{26} acyl-CoAs (Markham et al., 2011; Ternes et al., 2011; Luttgeharm et al., 2016). Class II (LOH1 and LOH3) ceramide synthase activity is essential for producing VLCFA-containing glycosphingolipids to support the growth of plant cells, whereas class I (LOH2) ceramide synthase activity is nonessential under normal growth conditions (Markham et al., 2011; Luttgeharm et al., 2015b). It was speculated recently that LOH2 ceramide synthase functions, in part, as a safety valve to acylate excess LCBs for glycosylation, resulting in a less cytotoxic form (Luttgeharm et al., 2015b; Msanne et al., 2015). Recent studies have shown that the Lag1/Lac1 components of the *S. cerevisiae* ceramide synthase are phosphorylated by Ypk1, and this phosphorylation stimulates ceramide synthase activity in response to heat and reduced intracellular sphingolipid levels (Muir et al., 2014). This finding points to possible coordinated regulation of ORM-mediated SPT and ceramide synthase activities to regulate sphingolipid homeostasis, which is likely more complicated in plants and mammals due to the occurrence of functionally distinct ceramide synthases in these systems (Stiban et al., 2010; Markham et al., 2011; Ternes et al., 2011; Luttgeharm et al., 2016).

RNA interference (RNAi) suppression of ORM genes in rice (*Oryza sativa*) has been shown to affect pollen viability (Chueasiri et al., 2014), but no mechanistic characterization of ORM proteins in plants has yet to be reported. Here, we describe two Arabidopsis ORMs, AtORM1 and AtORM2, that suppress SPT activity through direct interaction with the LCB1/LCB2 heterodimer. We also show that strong up-regulation of *AtORM* expression impairs growth. In addition, up- or down-regulation of ORMs is shown to differentially affect the sensitivity of Arabidopsis to the PCD-inducing mycotoxin fumonisin B_1 (FB_1), a ceramide synthase inhibitor, and to differentially affect the activities of class I and II ceramide synthases as a possible additional mechanism for regulating sphingolipid homeostasis.

RESULTS

Two Functional Homologs of Mammalian ORMDLs Interact Physically with and Inhibit Arabidopsis SPT

Two genes, designated *AtORM1* (At1g01230) and *AtORM2* (At5g42000), encoding 157- and 154-amino acid polypeptides, respectively, were identified in homology searches using human ORMDLs as a query (Hjelmqvist et al., 2002). The amino acid sequences of the Arabidopsis polypeptides share 81% identity and have predicted homologs throughout the plant kingdom. Arabidopsis ORM1 (AtORM1) and ORM2 (AtORM2) share 38% to 43% identity with human ORMDL1, ORMDL2, and ORMDL3. AtORM1 and AtORM2 also share 35% to 39% identity with *S. cerevisiae* ORM1 and ORM2 but, interestingly, lack the N-terminal phosphorylation domain found in the yeast ORMs (Fig. 1A). Notably, this N-terminal domain also is absent from ORMDL proteins from human and other mammals. Similar to the mammalian ORMDL proteins, AtORM1 and AtORM2 are predicted to have two,

three, or four transmembrane domains based on in silico analyses using the TopPred II, SOSUI, TMPred, MEMSAT, and DAS filter programs (von Heijne, 1992; Hirokawa et al., 1998). However, glycosylation cassettes (GCs) inserted at key sites along the yeast ORM2 protein support the presence of four transmembrane domains with the N and C termini residing in the cytosol (Fig. 1B). Given the significant homology between the yeast, plant, and human ORM proteins, it is likely that all members of the ORM family of proteins have the topology depicted in Figure 1C.

To test whether the AtORM polypeptides interact physically with AtSPT, FLAG-tagged AtLCB1 was expressed along with Myc-AtLCB2a, hemagglutinin (HA)-tagged AtssSPTa, and HA-tagged AtORM1 or AtORM2 in a yeast mutant that lacks endogenous SPT due to knockout of the yeast *LCB1* and *TSC3* genes. Pull-down assays using anti-FLAG antibodies with solubilized microsomes of cells expressing these polypeptides resulted in the detection of not only AtLCB1 but also AtLCB2a, AtssSPTa, AtORM1, or AtORM2 but no detection of ELO3, an ER polypeptide not known to

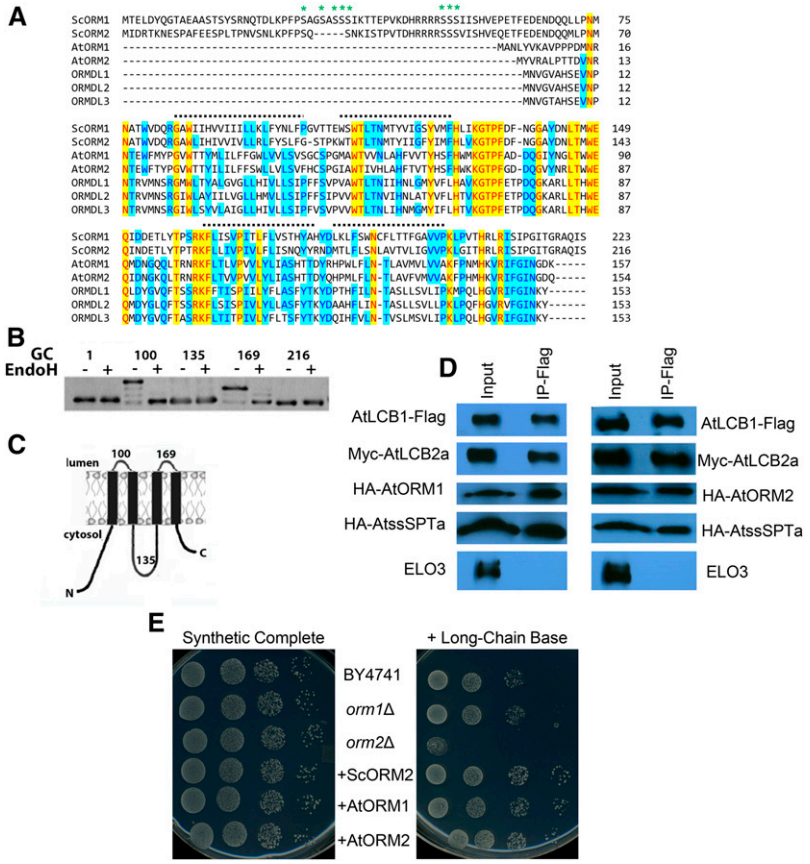

Figure 1. Arabidopsis ORMs interact physically with the Arabidopsis core SPT components and complement an *S. cerevisiae ORM2* knockout mutant. A, Amino acid sequence alignment for ORM polypeptides from *S. cerevisiae* (ScORM1 and ScORM2), Arabidopsis (AtORM1 and AtORM2), and *Homo sapiens* (ORMDL1, ORMDL2, and ORMDL3). The alignments show the N-terminal extension, found only in yeast, responsible for the reversible phosphorylation (at residues marked with asterisks) that modulates SPT activity (Breslow et al., 2010). The dotted lines mark the positions of four potential transmembrane domains identified by hydropathy analyses. B, Topology mapping of ScORM2. GCs were inserted after the indicated amino acids, and the GC-tagged proteins were expressed in yeast. Increased mobility following treatment of microsomes with endoglycosidase H (EndoH) revealed that the GCs at residues 100 and 169 are glycosylated and, therefore, reside in the lumen of the endoplasmic reticulum (ER). C, Model of ORM protein topology. The figure shows the experimentally determined membrane topology of ScORM2 as shown in B. D, Coimmunoprecipitation of FLAG-tagged AtLCB1 in yeast expressing AtLCB1-FLAG, AtLCB2a-Myc, AtssSPTa-HA, and either AtORM1-HA or AtORM2-HA. Solubilized yeast microsomes were incubated with anti-FLAG beads, and protein was eluted with FLAG peptide. Solubilized microsomes (Input) and the eluent (IP-Flag) were analyzed by SDS-PAGE, and the polypeptides were detected by immunoblotting. ELO3 was used as a negative control. E, *AtORM1* and *AtORM2* complement the sensitivity of the *S. cerevisiae orm2*Δ mutant to exogenous LCBs. Shown are plates containing synthetic complete medium lacking or supplemented with the LCB phytosphingosine at a concentration of 15 μM. As shown, plates contain dilutions of the parental cell line BY4741, *S. cerevisiae orm1*Δ mutant, *S. cerevisiae orm2*Δ mutant, and *S. cerevisiae orm2*Δ complemented with the wild-type copy of the *S. cerevisiae ORM2* (+ScORM2), *AtORM1* (+AtORM1), or *AtORM2* (+AtORM2).

associate with SPT (Fig. 1D). These results are consistent with the physical interaction of AtORM1 and AtORM2 with the core SPT complex.

To examine their ability to function as suppressors of SPT activity, Arabidopsis ORM1 and ORM2 were expressed in the *S. cerevisiae orm2*Δ mutant. The *orm2*Δ mutant in yeast has a strong sensitivity to excess LCB, and the inclusion of 15 μM phytosphingosine in medium is toxic to this mutant (Han et al., 2010). Expression of AtORM1 or AtORM2 in the *orm2*Δ mutant rescued the sensitivity of the mutant to exogenous LCB, consistent with the ability of the Arabidopsis proteins to suppress SPT activity (Fig. 1E). In addition, Arabidopsis ORM1 and ORM2 were coexpressed along with AtLCB1^{C144W}, AtLCB2a, and AtssSPTa in the yeast *lcb1Δtsc3Δ* mutant strain lacking endogenous SPT. AtLCB1^{C144W} contains a single amino acid substitution analogous to the HSAN1-causing mutation in human LCB1 (Gable et al., 2010). SPT containing the AtLCB1^{C144W} subunit condenses both Ser and Ala with palmitoyl-CoA to form normal LCB (d18:0) and deoxy-LCB (deoxy-sphinganine [DoxSA]; m18:0), respectively (Fig. 2A). Deoxy-LCBs cannot be degraded due to the missing hydroxyl group and serve as an in situ read out of SPT activity. When expressed in this background, Arabidopsis ORM1 and ORM2 markedly decreased the amount of deoxy-LCB produced, indicating that they act as SPT inhibitors (Fig. 2, B and C). The inhibitory effect of the AtORMs also was observed using native AtSPT expressed in a yeast mutant lacking endogenous SPT (Fig. 2D).

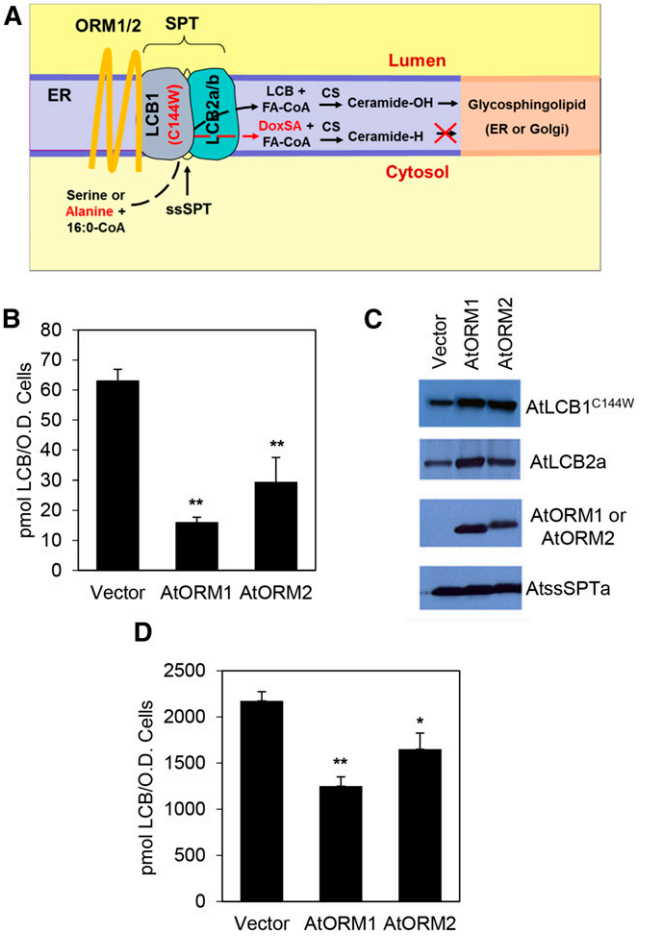

Figure 2. AtORM1 and AtORM2 are negative regulators of SPT activity. A, Schematic representation of the core SPT complex consisting of AtLCB1, AtLCB2a/b, AtssSPT, and AtORM. The complex resides in the ER membrane and catalyzes a condensation reaction between Ser and palmitoyl-CoA to produce LCB. The C144W (HSAN1) mutation in AtLCB1 allows SPT to use Ala as well as Ser as a substrate. The deoxy-LCB produced with Ala is referred to as DoxSA and lacks the hydroxyl group that is needed for LCB degradation and for conversion to the glycosphingolipid GlcCer in the ER or GIPC in the Golgi. B, In vivo AtSPT activity was measured in a yeast mutant that lacks endogenous SPT. Cells expressing AtLCB1^{C144W}, AtLCB2a, or AtssSPTa with or without AtORM1 or AtORM2 were used to demonstrate an inhibitory effect on SPT activity. The activity is measured by the accumulation of DoxSA, produced by the AtLCB1^{C144W}-containing mutant SPT enzyme. The DoxSA product is not produced naturally and is not degraded. Values shown are averages of three independent assays ± SD. **, $P < 0.01$. C, Immunoblot of yeast microsomes expressing AtLCB1^{C144W}-FLAG, AtLCB2a-Myc, AtORM1/2-HA, and AtssSPTa-HA. Anti-FLAG, anti-Myc, and anti-HA antibodies were used for detection. The results show that the C144W mutation in AtLCB1 does not affect the interaction of SPT components and interacting proteins. D, In vivo AtSPT activity measured in cells of yeast lacking endogenous SPT but expressing AtLCB1, AtLCB2a, AtssSPTa (Vector), and either AtORM1 or AtORM2. The activity is measured through the accumulation of total LCB produced. Values shown are averages of three independent assays ± SD. *, $P < 0.05$; and **, $P < 0.01$.

AtORM1 and AtORM2 Polypeptides Are ER Associated, and *AtORM1* and *AtORM2* Are Constitutively Expressed

The subcellular localization of ORM1 and ORM2 polypeptides was visualized using N-terminal and C-terminal yellow fluorescent protein (YFP) tags with transient expression in *Nicotiana benthamiana* (Fig. 3, A–F). Tagged ORM1 and ORM2 colocalized with the ER marker mCherry-HDEL (Fig. 3, C and F), consistent with the known ER localization of AtLCB1, AtLCB2a/2b, and AtssSPTa/b (Chen et al., 2006; Dietrich et al., 2008; Teng et al., 2008; Kimberlin et al., 2013), but also were detected in other subcellular locations, including the cytosol (Fig. 3, A, C, D, and F).

To assess the in planta contributions of each gene to SPT inhibition, transcript levels of *AtORM1* and *AtORM2* were measured in different organs of Arabidopsis. Our analyses revealed that the *AtORM1* transcript was approximately 3- to 4-fold more abundant in all tissues tested except pollen, whereas the *AtORM2* transcript was approximately 4-fold more abundant (Fig. 3G). Our results are broadly consistent with those for these genes in the AtGenExpress public microarray database (Supplemental Fig. S1).

Using *AtORM1* and *AtORM2* promoter::GUS fusion constructs, the location of in planta expression was examined. Promoters for both genes conferred expression in vegetative tissues, with GUS staining most pronounced in vascular tissues. Differences in promoter activity for *AtORM1* and *AtORM2* were observed in

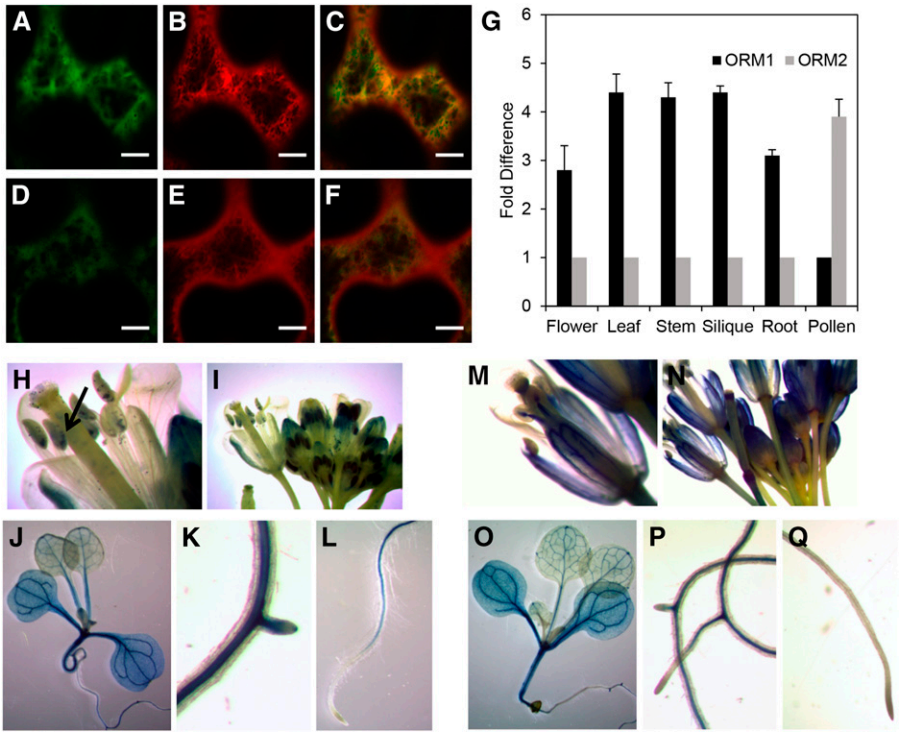

Figure 3. Subcellular localization of AtORM1 and AtORM2 polypeptides, and gene expression of *AtORM1* and *AtORM2* in Arabidopsis. A to F, Subcellular localization of AtORM1-YFP or AtORM2-YFP fusion coexpressed with the ER marker mCherry fusion construct. All constructs were transiently expressed in *N. benthamiana* through *Agrobacterium tumefaciens* infiltration and viewed by confocal microscopy. Green color in A and D shows AtORM1 and AtORM2 localization, respectively. The red color in B and E indicates ER marker localization. The yellow color seen in C and F indicates the colocalization of AtORM1 and AtORM2 polypeptides, respectively, with the ER marker. G, Relative expression of *AtORM1* and *AtORM2*. Tissues were collected from wild-type Columbia-0 (Col-0), and quantitative PCR (qPCR) was used to determine *AtORM1* and *AtORM2* transcript levels. *Protein phosphatase 2A subunit A3* (*PP2AA3*) was used as a reference gene. Values shown are means ± SD for three independent measurements and indicate relative fold increase of *AtORM1* or *AtORM2* compared with *AtORM2* or *AtORM1*, respectively. H to Q, *AtORM1* and *AtORM2* promoter::GUS expression analysis. An approximately 1-kb region upstream of the *AtORM1* (H–L) or *AtORM2* (M–Q) start codon was fused to the GUS gene and analyzed for expression in various organs and tissues as described previously (Jefferson et al., 1987). The arrow in H indicates the expression of *AtORM1* in developing embryos inside immature siliques.

floral tissues and roots. Based on the intensity of GUS staining, *AtORM1* promoter conferred higher expression in anthers and developing embryos than the *AtORM2* promoter (Fig. 3, H–J), while *AtORM2* promoter conferred greater expression than the *AtORM1* promoter in filaments, petals, sepals, pistils, and siliques (Fig. 3, M–O). Both *AtORM1* and *AtORM2* promoters yielded GUS expression in mature pollen grains and in roots. However, the *AtORM1* promoter, but not the *AtORM2* promoter, conferred detectable GUS expression in lateral root buds (Fig. 3, K, L, P, and Q).

Overexpression of *AtORM1* and *AtORM2* Results in Dwarfed Growth

To examine the in planta functions of *AtORM1* and *AtORM2*, three available T-DNA mutant lines for these genes were initially characterized: SALK_046054 (predicted T-DNA insertion in the first intron of *AtORM1*), GK-143A01 (predicted T-DNA insertion in the first exon of *AtORM1*), and SAIL_1286_D09 (predicted T-DNA insertion in the 5′ untranslated region of *AtORM2*). Homozygous lines were identified for each of these mutants, but full-length transcripts were still detected, indicating that these lines are not null mutants for the *AtORM1* and *AtORM2* genes (Supplemental Fig. S2). As an alternative approach for the characterization of the in planta functions of *AtORM1* and *AtORM2*, overexpression and RNAi suppression lines for these genes were created in Arabidopsis Col-0. Overexpression lines were prepared by placing the *AtORM1* or *AtORM2* cDNA under the control of the cauliflower mosaic virus 35S promoter. Homozygous lines were screened by qPCR to identify those with increased expression. A portion of the lines with confirmed overexpression of *AtORM1* or *AtORM2* were visually indistinguishable from Col-0 plants, including those with approximately 5-fold overexpression of *AtORM1* and approximately 35-fold overexpression of *AtORM2* in leaves (Fig. 4, B and E). However, a second class of overexpression lines for both genes was observed with

strong dwarfing. These lines included those with greater than 80-fold overexpression of *AtORM1* and approximately 800-fold overexpression of *AtORM2* in leaves relative to expression levels of these genes in Col-0 leaves (Fig. 4, C and F). These results suggest that a threshold of AtORM1 and AtORM2 protein levels can be reached to suppress SPT activity sufficiently to reduce growth, as observed previously for *AtLCB1* RNAi suppression (Chen et al., 2006) and reduced *AtssSPTa* expression (Kimberlin et al., 2013). Sphingolipidomic profiling revealed little quantitative difference between amounts of sphingolipids in Col-0 and *AtORM* overexpression lines and virtually no difference in amounts of sphingolipids between *AtORM* overexpression lines with or without a growth phenotype, especially in the GIPC and GlcCer classes (Supplemental Figs. S3–S6), similar to previous findings with *AtssSPT* overexpression or RNAi suppression (Kimberlin et al., 2013). It was notable that concentrations of the LCB t18:0 were elevated in ceramide and GIPC molecular species in dwarfed AtORM1 and AtORM2 plants compared with Col-0 control plants (Supplemental Fig. S3). *AtORM* RNAi suppression lines showed significant suppression of both *AtORM1* and *AtORM2* transcript (Supplemental Fig. S7). Consistent with a role of AtORMs as SPT repressors, SPT activity assayed from root microsomes of RNAi suppression lines showed increased SPT activity (Supplemental Fig. S8). No reductions in growth and no significant quantitative differences were seen in the sphingolipidome, particularly in GIPC and GlcCer amounts, in *AtORM* RNAi lines relative to the Col-0 controls (Supplemental Fig. S4–S6).

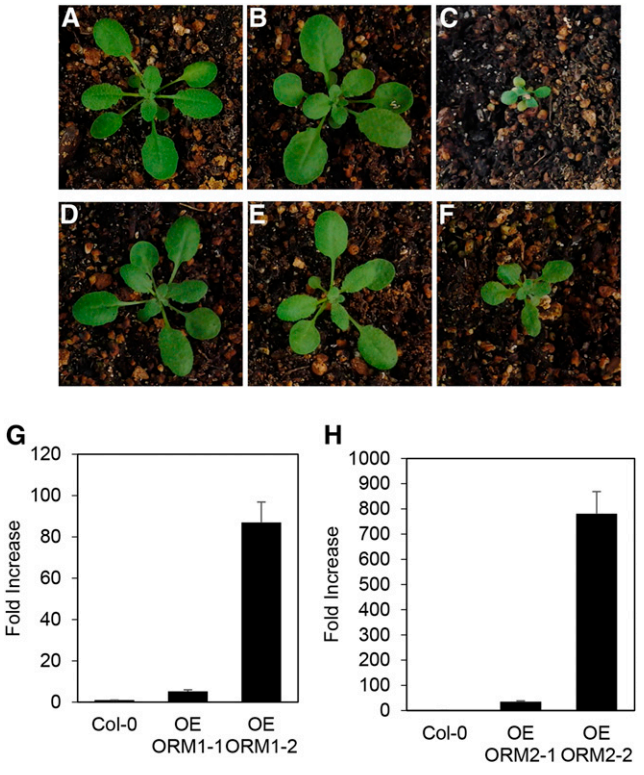

Figure 4. Phenotypes associated with *AtORM1* and *AtORM2* overexpression. A to F, High levels of *AtORM1* and *AtORM2* expression result in reduced plant size, early leaf senescence, and early plant death. Representative images of plants grown under the same conditions and of comparable age are shown. The wild type (Col-0) is shown in A and D. *AtORM1* overexpression line 1 (OE ORM1-1) is shown in B, while *AtORM2* overexpression line 1 (OE ORM2-1) is shown in E. *AtORM1* overexpression line 2 (OE ORM1-2) is shown in C, while *AtORM2* overexpression line 2 (OE ORM2-2) is shown in F. The phenotype correlates with ORM expression level, as lines with the strongest overexpression display a phenotype while relatively weaker overexpression lines do not show a noticeable growth phenotype. G and H, Expression levels of *AtORM1* (G) and *AtORM2* (H) in overexpressing lines (OE). Tissue was collected from wild-type Col-0 and lines overexpressing *AtORM1* and *AtORM2* grown under standard conditions. qPCR was used to determine relative *AtORM1* and *AtORM2* transcript levels by comparison with Col-0. *PP2AA3* was used as a reference gene. Values shown are means ± SD for three independent measurements and indicate relative fold increase of *AtORM1* or *AtORM2* compared with wild-type levels.

Modulation of *AtORM* Expression Affects Sensitivity to FB_1

The PCD-inducing mycotoxin FB_1, a ceramide synthase inhibitor, has been used routinely as a means of perturbing sphingolipid homeostasis for the study of SPT activity. From these studies, reduced SPT activity, such as that achieved by the suppression of *AtssSPTa*, results in enhanced resistance to FB_1 due presumably to reduced accumulation of cytotoxic LCBs (Kimberlin et al., 2013). Conversely, increased SPT activity, such as that obtained by the overexpression of *AtssSPTa*, results in enhanced sensitivity to FB_1 due presumably to the accumulation of cytotoxic LCBs (Kimberlin et al., 2013). Consistent with the suppression of SPT activity, *AtORM1* and *AtORM2* overexpression lines displayed increased resistance to FB_1, along with decreases in the accumulation of free LCBs and LCB phosphates (Fig. 5, A and B). These lines were viable at 0.5 μM FB_1, a concentration that was toxic to wild-type Arabidopsis (Fig. 5A). This phenotype was observed in a range of overexpression lines, including those with and without the dwarfing phenotype described above (Supplemental Fig. S8). Conversely, *AtORM* RNAi suppression lines were not viable on medium containing 0.3 μM FB_1, but no loss of viability was observed in wild-type plants at this concentration (Fig. 5A). RNAi suppression lines of *AtORM* were observed to have a large increase in free LCBs and LCB phosphates when grown on FB_1, which was particularly accentuated relative to AtORM overexpression lines and wild-type Col-0 on medium containing 0.5 μM FB_1 (Fig. 5B). Mirroring alterations in LCB concentrations in transgenic and wild-type plants in response to FB_1, concentrations of ceramides containing C16 fatty acids were lower in lines with overexpression of ORM and higher in RNAi suppression lines (Fig. 5C). These results indicate that altered *ORM* expression is an effective way of modulating plant

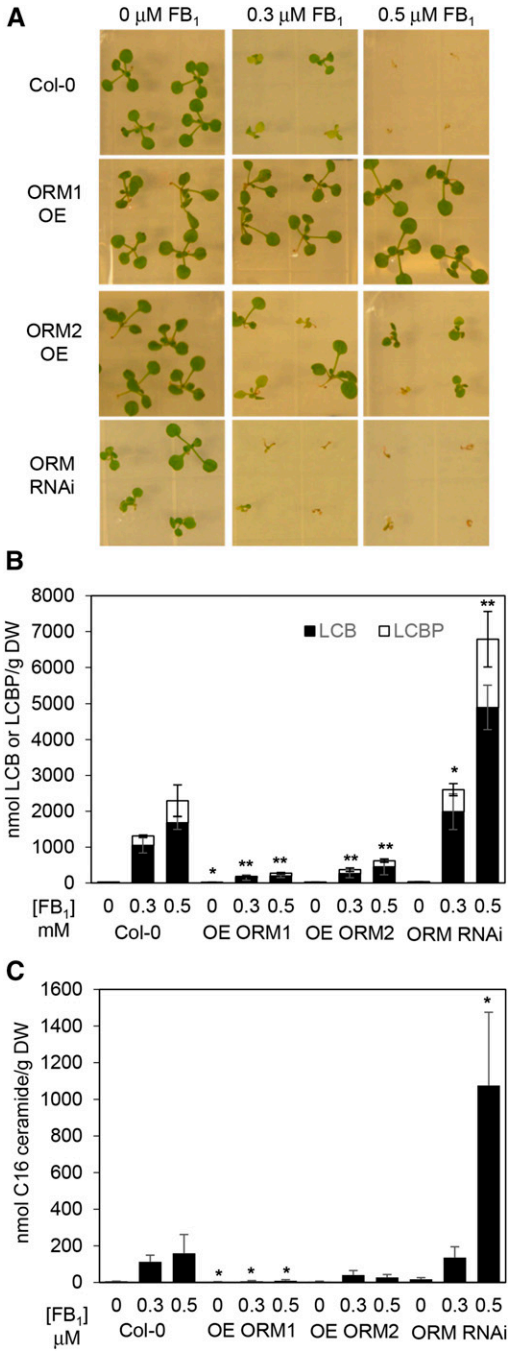

Figure 5. Modulation of *AtORM1* and *AtORM2* expression alters sensitivity to FB_1 and LCB as well as C16 ceramide accumulation. A, Altered *AtORM1* and *AtORM2* expression affects the sensitivity of plants to FB_1, a competitive inhibitor of ceramide synthase. Seeds were sown on Linsmaier and Skoog (LS) agar plates supplemented with FB_1 at 0.3 and 0.5 μM as indicated. The wild type (Col-0) is extremely sensitive to FB_1 at 0.5 μM and less affected at 0.3 μM. Up-regulation of *AtORM1* (ORM1) and *AtORM2* (ORM2) by transgenic overexpression (OE) causes an FB_1-resistant phenotype, whereas RNAi suppression of *AtORM* by RNAi causes an FB_1-sensitive phenotype (ORM RNAi). Images were taken 14 d after seeds were sown and are representative of three independent experiments. B, Altered *AtORM1* and *AtORM2* affects the accumulation of cytotoxic free LCB and LCB phosphate (LCBP) levels in response to FB_1 treatment. Wild-type plants show increased total LCB levels when treated with FB_1. Compared with the wild type, *AtORM1* and *AtORM2* overexpression plants display FB_1 resistance and reduced total LCB level. Alternatively, *AtORM* RNAi suppression plants display FB_1 sensitivity and increased total LCB level. Electrospray ionization-tandem mass spectrometry analyses were performed with three independent biological replicates ± SD. Plants were grown on LS plates ± FB_1 for 2 weeks before tissue collection. DW, Dry weight. *, $P < 0.05$; and **, $P < 0.01$. C, Total C16 ceramide levels are affected by the modulation of *AtORM* expression. *AtORM1* overexpression plants show decreased accumulation of C16 ceramide when compared with wild-type plants comparatively grown on LS plates ± FB_1, while ORM RNAi plants show increased accumulation of C16 ceramide. Analyses were performed as described in B with three independent biological replicates ± SD. *, $P < 0.05$.

sensitivity to FB_1 and indicate that AtORMs act as inhibitors of SPT.

Modulation of *AtORM* Expression Impacts Ceramide Synthase Activity

Recent studies in *S. cerevisiae* have suggested a role for ceramide synthase in the maintenance of sphingolipid homeostasis through a phosphorylation/dephosphorylation mechanism similar to that used for reversible modulation of ORMs (Muir et al., 2014). In contrast to *S. cerevisiae*, Arabidopsis has two functionally distinct ceramide synthase classes: class I and class II. This difference likely results in more complexity of potential ceramide synthase regulation of sphingolipid homeostasis in Arabidopsis. To gain insights into the coordinated regulation of ORMs and ceramide synthases, class I ceramide synthase was assayed in microsomes from roots of *AtORM1* and *AtORM2* overexpression lines and RNAi lines using 16:0-CoA and d18:0, the preferred substrates of this enzyme class. Class II ceramide synthase activity was assayed using 24:0-CoA and t18:0, preferred substrates of this enzyme class. Lower class I ceramide synthase activity was detected in microsomes of *AtORM1* and *AtORM2* overexpression lines, and increased activity was detected in microsomes from *AtORM* RNAi suppression lines (Fig. 6A). Conversely, class II ceramide synthase activity was decreased in microsomes from *AtORM* RNAi suppression lines but increased in *AtORM1* and *AtORM2* overexpression lines (Fig. 6B). These results suggest preferential metabolic flux through class I ceramide synthase for the synthesis of C16 fatty acid-containing ceramides with increased SPT activity resulting from disrupted ORM mediation of SPT in *AtORM* RNAi lines and preferential flux through class II ceramide synthases for the production of VLCFA-containing ceramides when SPT activity is limited by suppression from increased ORMs in *AtORM1* and *AtORM2* overexpression lines (Fig. 7). These findings are consistent with the increased concentrations of C16 fatty acid-containing ceramides

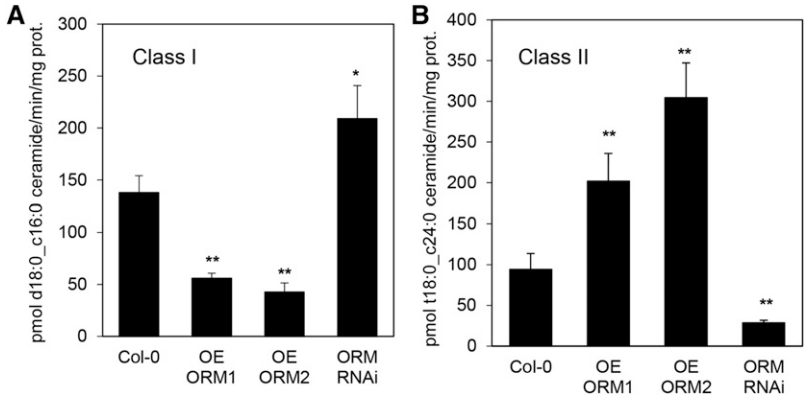

Figure 6. Ceramide synthase activity is altered by the modulation of *AtORM1* and *AtORM2* expression. A, Altered *AtORM1* and *AtORM2* expression affects class I ceramide synthase activity. Class I ceramide synthase activity was assayed on microsomal protein prepared from hydroponically grown root tissue using 16:0-CoA and d18:0 as substrates. Increases in *AtORM1* and *AtORM2* overexpression (OE ORM1, OE ORM2) resulted in decreases in class I ceramide synthase activity, while RNAi suppression of *AtORM* (ORM RNAi) resulted in an increase in activity of this enzyme. Analyses were performed with three independent biological replicates ± SD. *, $P < 0.05$; and **, $P < 0.01$. B, Increases in *AtORM1* (OE ORM1) and *AtORM2* (OE ORM2) expression resulted in increases in class II ceramide synthase activity, while RNAi suppression of *AtORM* resulted in a decrease in activity of this enzyme class. Activity assays were conducted with microsomes from hydroponically grown root tissue using 24:0-CoA and t18:0 substrates. Analyses were performed with three independent biological replicates ± SD. **, $P < 0.01$.

detected in *AtORM* RNAi lines in response to FB_1 treatment (Fig. 5C).

DISCUSSION

The findings reported here demonstrate the occurrence of two ORM proteins in Arabidopsis that share significant identity with human and yeast ORM polypeptides. We show that these polypeptides interact physically with a complex that includes AtLCB1/AtLCB2a and AtssSPTa. Consistent with a function as suppressors of SPT activity, the expression of AtORM1 and AtORM2 rescued the sensitivity of the yeast *orm2*Δ mutant to exogenous LCBs. Also consistent with a function as a suppressor of SPT activity, AtORM1 and AtORM2 inhibited SPT activity when overexpressed with the core Arabidopsis SPT components in a yeast mutant deficient in the native SPT and ORMs. Furthermore, overexpression of *AtORM1* and *AtORM2* resulted in enhanced resistance to FB_1, a phenotype also observed with reduced SPT activity associated with suppressed expression of *AtLCB1* (Shi et al., 2007), *AtLCB2* (Saucedo-García et al., 2011), or *AtssSPT* (Kimberlin et al., 2013). Moreover, RNAi-mediated down-regulation of *AtORM* expression resulted in increased sensitivity to FB_1, a phenotype also observed with increased SPT activity associated with the up-regulation of *AtssSPT* expression (Kimberlin et al., 2013). Altered *AtORM* expression also was accompanied by either enhanced accumulation of LCBs (*AtORM* RNAi lines) or reduced accumulation of LCBs (*AtORM* overexpression lines) relative to Col-0 controls in response to FB_1 treatment. These findings are consistent with altered SPT regulation in the ORM transgenic lines and with the function of AtORM1 and AtORM2 as negative regulators of SPT activity in Arabidopsis.

Also observed in parallel with these changes was enhanced accumulation of ceramides containing C16 fatty acids (*AtORM* RNAi lines) or reduced accumulation of ceramides containing C16 fatty acids (*AtORM* overexpression lines). These findings are consistent with the enhanced sequestration of LCBs as ceramides via the activity of ceramide synthase I (LOH2), which uses primarily C16 fatty acyl-CoAs as substrates, in response to deregulated SPT in *AtORM* RNAi lines. Also consistent with this, LOH2 activity was found to be increased significantly in microsomes from *AtORM* RNAi lines but decreased by more than 2-fold in *AtORM* overexpression lines compared with the Col-0 control. Unexpectedly, the opposite effect was observed in microsomes of these plants for class II ceramide synthase activity, which uses primarily trihydroxy LCBs and very-long-chain fatty acyl-CoAs as substrates: microsomes from *AtORM* RNAi lines had more than 3-fold less class II ceramide synthase activity, while microsomes for *AtORM* overexpression lines had more than 2-fold more activity of this enzyme class relative to the control. These findings point to coordinated control of the activities of the two functionally distinct ceramide synthase classes in response to altered ORM-mediated flux through SPT. As shown in Figure 7, we propose that the LOH2 ceramide synthase, a nonessential enzyme under normal growth conditions, provides a safety valve for excess LCB production, which is particularly accentuated in response to FB_1. As we have proposed previously, increased flux through LOH2 ceramide synthase may be coupled with GlcCer synthase activity to glucosylate C16 fatty acid-containing ceramides to a less cytotoxic form. Conversely, the

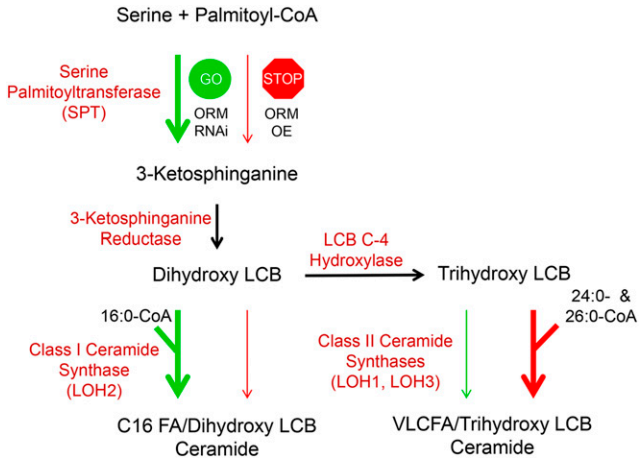

Figure 7. Model of the coordinated regulation of sphingolipid synthesis by AtORM1 and AtORM2 and ceramide synthase activity. The model represents the core synthesis pathway of ceramides in Arabidopsis. SPT catalyzes a condensation reaction between Ser and palmitoyl-CoA, leading to the production of 3-ketosphinganine, which is reduced to dihydroxy LCB (d18:0) through 3-ketosphinganine reductase activity. Dihydroxy LCBs can be used by class I ceramide synthase (LOH2) along with 16:0-CoA to produce C16 ceramides. Alternatively, dihydroxy LCBs can be hydroxylated by LCB C-4 hydroxylase to form trihydroxy LCBs (t18:0) that are used by class II ceramide synthases (LOH1 and LOH3) along with very long-chain fatty acyl-CoAs, primarily 24:0- and 26:0-CoA, to produce ceramides containing VLCFAs. In the model shown, modulation of *AtORM* expression leads to alterations in ceramide synthase activity. *AtORM* RNAi suppression, indicated by GO, results in increased SPT activity and increased generation of LCBs, with a concomitant increase in class I activity and a decrease in class II activity. Conversely, overexpression (OE) of *AtORM1* and *AtORM2*, indicated by STOP, results in decreased SPT activity and reduced LCB generation, with a concomitant decrease in class I activity and an increase in class II activity to ensure the production of sufficient levels of ceramides with VLCFAs to support growth. A role of LCB C-4 hydroxylase activity in mediating relative flux through class I and II ceramide synthases, particularly in response to enhanced LCB synthesis, also is possible.

down-regulation of SPT activity by *AtORM* overexpression may result in the directing of LCB flux toward the synthesis of ceramides containing trihydroxy LCBs and VLCFAs, via class II ceramide synthases, to support growth. One notable observation of this and similar studies is that perturbations in sphingolipid homeostasis are accentuated in the presence of FB_1. One possibility is that the C16 fatty acid-containing ceramides resulting from LOH2 activity in FB_1-treated plants deregulate SPT or dilute possible sphingolipid signals (e.g. ceramides containing VLCFAs) that typically provide homeostatic regulation of SPT.

How the apparent coordinated mediation of SPT and ceramide synthase activities by ORM is regulated is currently under investigation. One possibility is that class I and II ceramide synthases are differentially regulated by phosphorylation. It is known, for example, that the activity of the yeast Lag1/Lac1 ceramide synthase is subject to regulation by phosphorylation at residues Ser-23 and Ser-24 in Lag1 and Lac1 by Ypk1 (Muir et al., 2014) and at residues Ser-393, Ser-395, and Ser-397 near their C termini by casein kinase2 (Fresques et al., 2015). In the latter case, phosphorylation of Lag1 and Lac1 affects the localization of these polypeptides by disrupting their ER retrieval (Fresques et al., 2015). Similar to the yeast ceramide synthase, the AtLOH1 ceramide synthase has four experimentally confirmed phosphorylated Sers (Ser-295, Ser-300, Ser-302, and Ser-304; Nühse et al., 2004), and AtLOH2 has two experimentally confirmed phosphorylated Sers (Ser-289 and Ser-291; Nühse et al., 2004; Sugiyama et al., 2008). Like the yeast Lag1 and Lac1 polypeptides, these phosphorylated Ser residues are in the vicinity of the C termini of AtLOH1 and AtLOH2, near presumptive ER retrieval sequences. Although not experimentally verified, AtLOH3 also has Ser residues analogous to those in AtLOH1 near its C terminus. The influence of this phosphorylation on ceramide synthase activity and possible changes in phosphorylation of these polypeptides in response to altered ORM regulation of SPT are currently under study. Overall, our findings indicate that the regulation of sphingolipid homeostasis extends beyond SPT and is more complex in eukaryotic organisms with multiple, functionally distinct ceramide synthases than that found in *S. cerevisiae*, which has only one ceramide synthase type (Mullen et al., 2012).

Although our results clearly show that AtORM1 and AtORM2 function to suppress SPT activity, still unclear in plants and mammals is how ORMs reversibly regulate SPT in response to changes in intracellular sphingolipid levels. Absent from plant and mammalian ORMs is the N-terminal Ser-rich domain found in the yeast ScORM1 and ScORM2 polypeptides. Phosphorylation of Ser residues in this domain by Ypk1 relieves SPT inhibition in response to low intracellular sphingolipid levels (Breslow et al., 2010; Han et al., 2010; Roelants et al., 2011), and dephosphorylation of these residues by Cdc55 protein phosphatase 2A results in ORM suppression of SPT in response to excess intracellular sphingolipid levels (Sun et al., 2012). The lack of the regulatory domain in plant and mammalian ORMs does not preclude that other residues are subject to reversible posttranslational modifications (e.g. phosphorylation/dephosphorylation). Other possibilities include changes in ORM turnover rates or ORM localization in response to intracellular sphingolipid levels. With regard to the latter possibility, our localization studies showed that AtORM polypeptides are present primarily, but not exclusively, in the ER. As described above, changes in ER localization have been proposed as a component of yeast ceramide synthase activity (Fresques et al., 2015). More extensive studies, beyond the scope of those in this report, are currently under way to address this central question of how SPT is regulated to maintain intracellular homeostasis in plants and animals.

MATERIALS AND METHODS

Yeast Growth and Expression Plasmids

Yeast (*Saccharomyces cerevisiae*) strain TDY9113 (Mata *tsc3*Δ:NAT *lcb1*Δ:KAN *ura3 leu2 lys2 trp1*Δ) lacking endogenous SPT was used for the expression and characterization of Arabidopsis (*Arabidopsis thaliana*) SPT subunits and ORM proteins. The mutant was cultured in medium containing 15 μM phytosphingosine and 0.2% (w/v) Tergitol Nonidet P-40. The *AtORM1* (At1g01230) and *AtORM2* (At5g42000) open reading frames were amplified by PCR and inserted into pPR3-N (Dualsystems Biotech) for expression with N-terminal HA tags. pAL2-URA was constructed for divergent constitutive expression of AtLCB1-FLAG (or AtLCB1^{C144W}-FLAG) and Myc-tagged AtLCB2a by replacing the *GAL1* and *GAL10* promoters of pESC-URA (Stratagene) with the yeast *LCB2* and *ADH* promoters, respectively. The AtssSPTa cDNA open reading frame was inserted after the 3× HA tag in pADH1 (Kohlwein et al., 2001; Kimberlin et al., 2013).

Immunoprecipitation

Immunoprecipitation was conducted as described (Kimberlin et al., 2013) with minor modifications. Microsomal membrane proteins were prepared from yeast cells expressing FLAG-tagged AtLCB1 (or AtLCB1^{C144W}), Myc-tagged AtLCB2a, HA-tagged AtssSPTa, and HA-tagged AtORM1 or AtORM2. Microsomal membrane proteins were solubilized in 1.5% digitonin at 4°C for 2.5 h and incubated with Flag-beads (Sigma-Aldrich) overnight. The bound proteins were eluted in immunoprecipitation buffer (50 mM HEPES-KOH, pH 6.8, 150 mM potassium acetate, 2 mM magnesium acetate, 1 mM calcium chloride, and 15% glycerol) containing 0.25% digitonin and 200 μg mL^{-1} FLAG peptide, resolved on a 4% to 12% BisTris NuPAGE gel (Invitrogen), and detected by immunoblotting with anti-HA (Covance; 1:5,000 dilution), anti-Myc (Sigma-Aldrich; 1:3,000 dilution), and anti-FLAG (GenScript; 1:5,000 dilution) antibodies.

LCB Extraction and Analysis

LCBs were extracted, derivatized, and analyzed by reverse-phase HPLC as described previously (Gable et al., 2010). For measurement of LCBs and DoxSA formation, the areas under HPLC peaks, measured in luminescence units, were normalized to the internal C17 sphingosine standard, and the amounts of LCBs and 1-DoxSA were determined using standard curves for each of the LCBs and are reported as nmol LCBs per optical density of cells measured at 600 nm (Gable et al., 2010).

SPT Assay

Plant microsomes were prepared and SPT activity was assayed as described (Kimberlin et al., 2013), except that 50 μM palmitoyl-CoA and 20 μM bovine serum albumin were used for the Arabidopsis microsomal SPT assays. SPT activity was measured using the substrates [^{3}H]Ser and 16:0-CoA as described (Han et al., 2009).

Yeast Complementation

Synthetic complete medium was used to grow yeast (BY4741). Synthetic complete medium was supplemented with 15 μM phytosphingosine and 0.1% Tergitol. Yeast knockout mutants, *orm1Δ* and *orm2Δ*, were obtained from the *S. cerevisiae* knockout library kindly provided by Jaekwon Lee. *AtORM1* and *AtORM2* cDNAs were cloned into the centromeric plasmid pSH15 using the *Xho*I and *Pst*I restriction sites using primers P1 to P4 (Supplemental Table S1). The plasmid, pSH15, containing native *S. cerevisiae ORM2* was a gift from Dr. Amy Chang. Cells were grown at 30°C and then normalized to an optical density at 600 nm = 0.1 before being serially diluted and plated.

Plant Material and Growth Conditions

All Arabidopsis Col-0 lines used in this study were stratified at 4°C for 4 d and maintained at 22°C with a 16-h-light (100 μmol m^{-2} s^{-1})/8-h-dark cycle. Plants sown on LS agar plates were surface sterilized before stratification. Plants that were grown hydroponically were maintained on modified Hoagland solution as described previously in custom-made hydroponics tanks (Conn et al., 2013).

Arabidopsis Transformation and Selection

Binary vectors were transformed into *Agrobacterium tumefaciens* GV3101 by electroporation. The floral dip method was used to create transgenic plants in Arabidopsis Col-0 (Clough and Bent, 1998). A green light-emitting diode flashlight and a Red 2 camera filter were used to identify transformed seeds by fluorescence of the DsRed marker protein.

RNA Isolation and qPCR

For expression analyses of *AtORM1* and *AtORM2*, RNA extraction was done using the RNeasy Plant Kit (Qiagen) according to the manufacturer's protocol. RNA (1 μg) was treated with DNaseI (Invitrogen) according to the manufacturer's protocol. Treated RNA was then reverse transcribed to cDNA with the iScript cDNA synthesis kit (Bio-Rad) according to the manufacturer's protocol. For tissue-specific expression analysis, 6- to 8-week-old Col-0 plants were used as sources of plant material. qPCR was performed on cDNA using the Bio-Rad MyiQ iCycler qPCR instrument. Values shown are averages of three independent measurements ± SD. SYBR Green was used as the fluorophore in a qPCR supermix (Qiagen). QuantiTect (Qiagen) primer sets P5 to P7 (Supplemental Table S1) were used for relative quantification. *PP2AA3* (At1g13320) was used as an internal reference gene. Reverse transcription-PCR analysis of homozygous T-DNA mutant lines was performed on cDNA using primers P8 to P11 (Supplemental Table S1).

Analysis of Promoter GUS-Expressing Plants

To generate the *AtORM1* promoter::GUS and *AtORM2* promoter::GUS constructs, an approximately 1-kb region upstream of the start codon was PCR amplified from genomic DNA (oligonucleotides P12–P15; Supplemental Table S1) and cloned into a pBinGlyRed2 vector containing the GUS gene using the *Bam*HI and *Eco*RI restriction sites. This vector was then transformed into *A. tumefaciens* C58, and cells harboring the binary vector were used to transform wild-type Arabidopsis as described previously (Clough and Bent, 1998). GUS staining solution was composed of 20 mM sodium phosphate (monobasic), 30 mM sodium phosphate (dibasic), 2 mM potassium ferricyanide, and 2 mM potassium ferrocyanide, along with 1 μL mL^{-1} Triton X-100 and 1 mg mL^{-1} 5-bromo-4-chloro-3-indolyl-β-D-glucuronide. Tissues were preincubated in chilled 90% acetone for 10 min, then vacuum infiltrated with chilled GUS staining solution for 10 min. The tissues were incubated overnight at 37°C and then cleared with 100% ethanol followed by 70% ethanol. Images of GUS-analyzed tissue were taken with an Olympus AX70 optical microscope.

Subcellular Localization of ORM1 and ORM2

YFP fusion proteins with AtORM1 and AtORM2 were prepared by amplification of the *AtORM1* and *AtORM2* open reading frames using gene-specific primers (P16–P19; Supplemental Table S1). PCR products were cloned into the 35S-pFAST-eYFP vector using the *Sac*I and *Kpn*I restriction sites generating C-terminal YFP fusion constructs. *A. tumefaciens*-mediated infiltration of *Nicotiana benthamiana* leaves was performed with ORM1-YFP and ORM2-YFP constructs separately and in conjunction with the ER marker CD3-959 (HDEL-mCherry). Sequential imaging was performed using a Nikon A1 confocal imaging system mounted on a Nikon Eclipse 90i microscope. Excitation/emission wavelengths for YFP and mCherry were 488 nm/500 to 550 nm and 561.6 nm/570 to 620 nm, respectively, as described previously (Kimberlin et al., 2013).

Arabidopsis Mutant Genotyping

T-DNA insertion mutants were acquired from the Arabidopsis Biological Resource Center and the GABI-Kat collections. The REDextract-N-Amp Tissue PCR kit (Sigma-Aldrich) was used to extract genomic DNA from leaf tissue. Genotyping was performed by PCR using gene-specific and T-DNA-specific primer sets P20 to P28 (Supplemental Table S1).

Membrane Topology Mapping of ScORM2

The topology of ScORM2 protein was mapped based on the previously described methodology (Han et al., 2004). In brief, *Nhe*I restriction sites were created before codons for amino acids 2, 100, 135, and 169 and an *Xba*I site

before the stop codon (217) by use of the QuikChange mutagenesis kit (Agilent Technology). A GC encoding the 53-amino acid domain of invertase (Suc2p) was inserted into the *Nhe*I or *Xba*I site. The microsomal proteins were isolated from the strains transformed with the GC topology reporter plasmids and treated with endoglycosidase H. The proteins were resolved using a 4% to 12% BisTris NuPAGE gel system (Invitrogen).

FB_1 Screening of Arabidopsis *ORM1* and *ORM2* Overexpression and RNAi lines

ORM-overexpressing plants were generated by transforming Col-0 with the cauliflower mosaic virus 35S promoter:*ORM* cDNA constructs. *AtORM1* and *AtORM2* cDNAs were cloned into the binary vector pBinGlyRed3-35S using the *Eco*RI/*Xba*I restriction sites (P29–P32; Supplemental Table S1). *ORM* RNAi lines were generated by overexpressing a hairpin composed of an *AtORM1* or *AtORM2* gene fragment. The *ORM* gene fragments were cloned into the pINTRON vector using the *Xba*I, *Xho*I, *Spe*I, and *Hin*dIII restriction sites forming a hairpin using primers P33 to P36 (Supplemental Table S1). The pINTRON fragment containing the hairpin was amplified using primers P37 and P38 (Supplemental Table S1) and cloned into pBinGlyRed3-35S using the *Eco*RI/*Xba*I restriction sites. Arabidopsis (Col-0) plants were transformed with these constructs, and the resulting transformants were selected and screened by qPCR for *AtORM1* and *AtORM2* expression. Sensitivity screening relative to a wild-type control was done at 0, 0.3, and 0.5 μM FB_1 (Sigma-Aldrich) concentrations in LS medium. Sensitivity was determined by plant growth rate and germination at the varying FB_1 concentrations (Kimberlin et al., 2013). Plants were grown for 2 weeks on FB_1 before analysis.

Plant Microsomal Membrane Isolation

Microsomal membrane isolation from hydroponically grown 4-week-old Arabidopsis roots was performed as described previously (Lynch and Fairfield, 1993), and protein concentration was measured using the bicinchoninic acid method (Smith et al., 1985; Lynch and Fairfield, 1993).

Generation of the $AtLCB1^{C144W}$ Mutant

The C144W mutation was introduced into AtLCB1 by changing codon 144 TGT to TGG by QuikChange mutagenesis (Stratagene) using oligonucleotide primers P39 and P40 (Supplemental Table S1). The mutation was confirmed by sequencing.

Ceramide Synthase Assays

Ceramide synthase assays were performed on microsomal extracts (10 μg of protein) derived from hydroponically grown root using a previously described methodology (Luttgeharm et al., 2015a, 2016). Reaction substrates for class I ceramide synthase assays were d18:0 LCB and 16:0-CoA, while substrates for class II ceramide synthase assays were t18:0 LCB and 24:0-CoA. After incubation and extraction, sphingolipids produced in the assay were analyzed by mass spectrometry as described (Luttgeharm et al., 2015a, 2016).

Sphingolipid Analysis

Sphingolipids were extracted from 2 to 15 mg of lyophilized plant material and analyzed by liquid chromatography-tandem mass spectrometry as described previously (Markham and Jaworski, 2007; Kimberlin et al., 2013).

Supplemental Data

The following supplemental materials are available.

Supplemental Figure S1. Gene expression levels for *AtORM1* (At1g01230) and *AtORM2* (At5g42000) in different tissue types.

Supplemental Figure S2. Genotyping of T-DNA mutants for *AtORM1* and *AtORM2*.

Supplemental Figure S3. Sphingolipid profile of *AtORM1* and *AtORM2* overexpression lines that display the dwarf phenotype.

Supplemental Figure S4. Ceramide profile for Col-0 and *AtORM* overexpression and RNAi lines grown on LS medium ± FB_1.

Supplemental Figure S5. GlcCer profile for Col-0 and *AtORM* overexpression and RNAi lines grown on LS medium ± FB_1.

Supplemental Figure S6. GIPC profile for Col-0 and *AtORM* overexpression and RNAi lines grown on LS medium ± FB_1.

Supplemental Figure S7. qPCR analysis of ORM RNAi lines.

Supplemental Figure S8. SPT activity from root microsomes of wild-type and transgenic plants.

Supplemental Table S1. Oligonucleotide primers used in the reported studies.

ACKNOWLEDGMENTS

We thank Amy Chang (University of Michigan) for providing plasmid pSH15 containing *S. cerevisiae ORM2* and Jaekwon Lee (University of Nebraska-Lincoln) for providing *S. cerevisiae* knockout lines for *ORM1* and *ORM2*.

Received June 15, 2016; accepted August 5, 2016; published August 9, 2016.

LITERATURE CITED

Bach L, Gissot L, Marion J, Tellier F, Moreau P, Satiat-Jeunemaître B, Palauqui JC, Napier JA, Faure JD (2011) Very-long-chain fatty acids are required for cell plate formation during cytokinesis in *Arabidopsis thaliana*. J Cell Sci **124:** 3223–3234

Bach L, Michaelson LV, Haslam R, Bellec Y, Gissot L, Marion J, Da Costa M, Boutin JP, Miquel M, Tellier F, et al (2008) The very-long-chain hydroxy fatty acyl-CoA dehydratase *PASTICCINO2* is essential and limiting for plant development. Proc Natl Acad Sci USA **105:** 14727–14731

Bayer EM, Mongrand S, Tilsner J (2014) Specialized membrane domains of plasmodesmata, plant intercellular nanopores. Front Plant Sci **5:** 507

Bi FC, Liu Z, Wu JX, Liang H, Xi XL, Fang C, Sun TJ, Yin J, Dai GY, Rong C, et al (2014) Loss of ceramide kinase in *Arabidopsis* impairs defenses and promotes ceramide accumulation and mitochondrial H_2O_2 bursts. Plant Cell **26:** 3449–3467

Breslow DK (2013) Sphingolipid homeostasis in the endoplasmic reticulum and beyond. Cold Spring Harb Perspect Biol **5:** a013326

Breslow DK, Collins SR, Bodenmiller B, Aebersold R, Simons K, Shevchenko A, Ejsing CS, Weissman JS (2010) *Orm* family proteins mediate sphingolipid homeostasis. Nature **463:** 1048–1053

Cacas JL, Buré C, Grosjean K, Gerbeau-Pissot P, Lherminier J, Rombouts Y, Maes E, Bossard C, Gronnier J, Furt F, et al (2016) Revisiting plant plasma membrane lipids in tobacco: a focus on sphingolipids. Plant Physiol **170:** 367–384

Cacas JL, Furt F, Le Guédard M, Schmitter JM, Buré C, Gerbeau-Pissot P, Moreau P, Bessoule JJ, Simon-Plas F, Mongrand S (2012) Lipids of plant membrane rafts. Prog Lipid Res **51:** 272–299

Chen M, Han G, Dietrich CR, Dunn TM, Cahoon EB (2006) The essential nature of sphingolipids in plants as revealed by the functional identification and characterization of the *Arabidopsis* LCB1 subunit of serine palmitoyltransferase. Plant Cell **18:** 3576–3593

Chen M, Markham JE, Dietrich CR, Jaworski JG, Cahoon EB (2008) Sphingolipid long-chain base hydroxylation is important for growth and regulation of sphingolipid content and composition in *Arabidopsis*. Plant Cell **20:** 1862–1878

Chueasiri C, Chunthong K, Pitnjam K, Chakhonkaen S, Sangarwut N, Sangsawang K, Suksangpanomrung M, Michaelson LV, Napier JA, Muangprom A (2014) Rice ORMDL controls sphingolipid homeostasis affecting fertility resulting from abnormal pollen development. PLoS ONE **9:** e106386

Clough SJ, Bent AF (1998) Floral dip: a simplified method for Agrobacterium-mediated transformation of Arabidopsis thaliana. Plant J **16:** 735–743

Conn SJ, Hocking B, Dayod M, Xu B, Athman A, Henderson S, Aukett L, Conn V, Shearer MK, Fuentes S, et al (2013) Protocol: optimising hydroponic growth systems for nutritional and physiological analysis of Arabidopsis thaliana and other plants. Plant Methods **9:** 4

Dietrich CR, Han G, Chen M, Berg RH, Dunn TM, Cahoon EB (2008) Loss-of-function mutations and inducible RNAi suppression of

Arabidopsis LCB2 genes reveal the critical role of sphingolipids in gametophytic and sporophytic cell viability. Plant J **54:** 284–298

Fresques T, Niles B, Aronova S, Mogri H, Rakhshandehroo T, Powers T (2015) Regulation of ceramide synthase by casein kinase 2-dependent phosphorylation in Saccharomyces cerevisiae. J Biol Chem **290:** 1395–1403

Gable K, Gupta SD, Han G, Niranjanakumari S, Harmon JM, Dunn TM (2010) A disease-causing mutation in the active site of serine palmitoyltransferase causes catalytic promiscuity. J Biol Chem **285:** 22846–22852

Greenberg JT, Silverman FP, Liang H (2000) Uncoupling salicylic acid-dependent cell death and defense-related responses from disease resistance in the Arabidopsis mutant *acd5*. Genetics **156:** 341–350

Gururaj C, Federman RS, Chang A (2013) Orm proteins integrate multiple signals to maintain sphingolipid homeostasis. J Biol Chem **288:** 20453–20463

Han G, Gable K, Yan L, Natarajan M, Krishnamurthy J, Gupta SD, Borovitskaya A, Harmon JM, Dunn TM (2004) The topology of the Lcb1p subunit of yeast serine palmitoyltransferase. J Biol Chem **279:** 53707–53716

Han G, Gupta SD, Gable K, Niranjanakumari S, Moitra P, Eichler F, Brown RH Jr, Harmon JM, Dunn TM (2009) Identification of small subunits of mammalian serine palmitoyltransferase that confer distinct acyl-CoA substrate specificities. Proc Natl Acad Sci USA **106:** 8186–8191

Han S, Lone MA, Schneiter R, Chang A (2010) Orm1 and Orm2 are conserved endoplasmic reticulum membrane proteins regulating lipid homeostasis and protein quality control. Proc Natl Acad Sci USA **107:** 5851–5856

Hanada K (2003) Serine palmitoyltransferase, a key enzyme of sphingolipid metabolism. Biochim Biophys Acta **1632:** 16–30

Hirokawa T, Boon-Chieng S, Mitaku S (1998) SOSUI: classification and secondary structure prediction system for membrane proteins. Bioinformatics **14:** 378–379

Hjelmqvist L, Tuson M, Marfany G, Herrero E, Balcells S, Gonzalez-Duarte R (2002) ORMDL proteins are a conserved new family of endoplasmic reticulum membrane proteins. Genome Biol **3:** RESEARCH0027

Jefferson RA, Kavanagh TA, Bevan MW (1987) GUS fusions: beta-glucuronidase as a sensitive and versatile gene fusion marker in higher plants. EMBO J **6:** 3901–3907

Kimberlin AN, Majumder S, Han G, Chen M, Cahoon RE, Stone JM, Dunn TM, Cahoon EB (2013) *Arabidopsis* 56-amino acid serine palmitoyltransferase-interacting proteins stimulate sphingolipid synthesis, are essential, and affect mycotoxin sensitivity. Plant Cell **25:** 4627–4639

Kohlwein SD, Eder S, Oh CS, Martin CE, Gable K, Bacikova D, Dunn T (2001) Tsc13p is required for fatty acid elongation and localizes to a novel structure at the nuclear-vacuolar interface in Saccharomyces cerevisiae. Mol Cell Biol **21:** 109–125

Liang H, Yao N, Song JT, Luo S, Lu H, Greenberg JT (2003) Ceramides modulate programmed cell death in plants. Genes Dev **17:** 2636–2641

Luttgeharm KD, Cahoon EB, Markham JE (2015a) A mass spectrometry-based method for the assay of ceramide synthase substrate specificity. Anal Biochem **478:** 96–101

Luttgeharm KD, Cahoon EB, Markham JE (2016) Substrate specificity, kinetic properties and inhibition by fumonisin B_1 of ceramide synthase isoforms from Arabidopsis. Biochem J **473:** 593–603

Luttgeharm KD, Chen M, Mehra A, Cahoon RE, Markham JE, Cahoon EB (2015b) Overexpression of Arabidopsis ceramide synthases differentially affects growth, sphingolipid metabolism, programmed cell death, and mycotoxin resistance. Plant Physiol **169:** 1108–1117

Lynch DV, Fairfield SR (1993) Sphingolipid long-chain base synthesis in plants: characterization of serine palmitoyltransferase activity in squash fruit microsomes. Plant Physiol **103:** 1421–1429

Markham JE, Jaworski JG (2007) Rapid measurement of sphingolipids from *Arabidopsis thaliana* by reversed-phase high-performance liquid chromatography coupled to electrospray ionization tandem mass spectrometry. Rapid Commun Mass Spectrom **21:** 1304–1314

Markham JE, Lynch DV, Napier JA, Dunn TM, Cahoon EB (2013) Plant sphingolipids: function follows form. Curr Opin Plant Biol **16:** 350–357

Markham JE, Molino D, Gissot L, Bellec Y, Hématy K, Marion J, Belcram K, Palauqui JC, Satiat-Jeunemaître B, Faure JD (2011) Sphingolipids containing very-long-chain fatty acids define a secretory pathway for specific polar plasma membrane protein targeting in *Arabidopsis*. Plant Cell **23:** 2362–2378

Melser S, Molino D, Batailler B, Peypelut M, Laloi M, Wattelet-Boyer V, Bellec Y, Faure JD, Moreau P (2011) Links between lipid homeostasis, organelle morphodynamics and protein trafficking in eukaryotic and plant secretory pathways. Plant Cell Rep **30:** 177–193

Msanne J, Chen M, Luttgeharm KD, Bradley AM, Mays ES, Paper JM, Boyle DL, Cahoon RE, Schrick K, Cahoon EB (2015) Glucosylceramides are critical for cell-type differentiation and organogenesis, but not for cell viability in Arabidopsis. Plant J **84:** 188–201

Muir A, Ramachandran S, Roelants FM, Timmons G, Thorner J (2014) TORC2-dependent protein kinase Ypk1 phosphorylates ceramide synthase to stimulate synthesis of complex sphingolipids. eLife **3:** 3

Mullen TD, Hannun YA, Obeid LM (2012) Ceramide synthases at the centre of sphingolipid metabolism and biology. Biochem J **441:** 789–802

Nühse TS, Stensballe A, Jensen ON, Peck SC (2004) Phosphoproteomics of the *Arabidopsis* plasma membrane and a new phosphorylation site database. Plant Cell **16:** 2394–2405

Perraki A, Cacas JL, Crowet JM, Lins L, Castroviejo M, German-Retana S, Mongrand S, Raffaele S (2012) Plasma membrane localization of *Solanum tuberosum* remorin from group 1, homolog 3 is mediated by conformational changes in a novel C-terminal anchor and required for the restriction of potato virus X movement. Plant Physiol **160:** 624–637

Roelants FM, Breslow DK, Muir A, Weissman JS, Thorner J (2011) Protein kinase Ypk1 phosphorylates regulatory proteins Orm1 and Orm2 to control sphingolipid homeostasis in Saccharomyces cerevisiae. Proc Natl Acad Sci USA **108:** 19222–19227

Saucedo-García M, Guevara-García A, González-Solís A, Cruz-García F, Vázquez-Santana S, Markham JE, Lozano-Rosas MG, Dietrich CR, Ramos-Vega M, Cahoon EB, et al (2011) MPK6, sphinganine and the LCB2a gene from serine palmitoyltransferase are required in the signaling pathway that mediates cell death induced by long chain bases in Arabidopsis. New Phytol **191:** 943–957

Shi L, Bielawski J, Mu J, Dong H, Teng C, Zhang J, Yang X, Tomishige N, Hanada K, Hannun YA, et al (2007) Involvement of sphingoid bases in mediating reactive oxygen intermediate production and programmed cell death in Arabidopsis. Cell Res **17:** 1030–1040

Simanshu DK, Zhai X, Munch D, Hofius D, Markham JE, Bielawski J, Bielawska A, Malinina L, Molotkovsky JG, Mundy JW, et al (2014) Arabidopsis *accelerated cell death 11*, *ACD11*, is a ceramide-1-phosphate transfer protein and intermediary regulator of phytoceramide levels. Cell Rep **6:** 388–399

Smith PK, Krohn RI, Hermanson GT, Mallia AK, Gartner FH, Provenzano MD, Fujimoto EK, Goeke NM, Olson BJ, Klenk DC (1985) Measurement of protein using bicinchoninic acid. Anal Biochem **150:** 76–85

Sperling P, Franke S, Lüthje S, Heinz E (2005) Are glucocerebrosides the predominant sphingolipids in plant plasma membranes? Plant Physiol Biochem **43:** 1031–1038

Stiban J, Tidhar R, Futerman AH (2010) Ceramide synthases: roles in cell physiology and signaling. Adv Exp Med Biol **688:** 60–71

Sugiyama N, Nakagami H, Mochida K, Daudi A, Tomita M, Shirasu K, Ishihama Y (2008) Large-scale phosphorylation mapping reveals the extent of tyrosine phosphorylation in Arabidopsis. Mol Syst Biol **4:** 193

Sun Y, Miao Y, Yamane Y, Zhang C, Shokat KM, Takematsu H, Kozutsumi Y, Drubin DG (2012) Orm protein phosphoregulation mediates transient sphingolipid biosynthesis response to heat stress via the Pkh-Ypk and Cdc55-PP2A pathways. Mol Biol Cell **23:** 2388–2398

Teng C, Dong H, Shi L, Deng Y, Mu J, Zhang J, Yang X, Zuo J (2008) Serine palmitoyltransferase, a key enzyme for de novo synthesis of sphingolipids, is essential for male gametophyte development in Arabidopsis. Plant Physiol **146:** 1322–1332

Ternes P, Feussner K, Werner S, Lerche J, Iven T, Heilmann I, Riezman H, Feussner I (2011) Disruption of the ceramide synthase LOH1 causes spontaneous cell death in *Arabidopsis thaliana*. New Phytol **192:** 841–854

von Heijne G (1992) Membrane protein structure prediction: hydrophobicity analysis and the positive-inside rule. J Mol Biol **225:** 487–494